Benzofurans from *Styrax agrestis* As Acetylcholinesterase Inhibitors: Structure−Activity Relationships and Molecular Modeling Studies

Jiawei Liu,[†,‡] Vincent Dumontet,*,[‡] Anne-Laure Simonin,[‡] Bogdan I. Iorga,[‡] Vincent Guerineau,[‡] Marc Litaudon,[‡] Van Hung Nguyen,[§] and Françoise Gueritte[‡]

[†]Research Center of Medicinal Plants Resource Science and Engineering, Guangzhou University of Chinese Medicine, 232 Waihuandong Road, Higher Education Mega Center, Guangzhou 510006, People's Republic of China

[‡]Centre de Recherche de Gif, Institut de Chimie des Substances Naturelles, CNRS, Bâtiment 27, Avenue de la Terrasse, CNRS, 91198 Gif-sur-Yvette, France

[§]Institute of Chemistry, VAST, 18 Hoang Quoc Viet Street, Cau Giay District, Hanoi, Vietnam

Ⓢ *Supporting Information*

ABSTRACT: An extract of *Styrax agrestis* fruits, collected in Vietnam, significantly inhibited acetylcholinesterase (AChE) in vitro. Bioassay-guided fractionation revealed three new egonol-type benzofurans: egonol-9(*Z*),12(*Z*) linoleate (**1**), 7-demethoxy-egonol-9(*Z*),12(*Z*) linoleate (**2**), and 7-demethoxyegonol oleate (**4**). Ten known egonol-type benzofurans were also isolated (**3**, **5**, **6**−**13**). In order to better understand structure−activity relationships in this series, egonol derivatives **14**−**19** were prepared by chemical modifications and evaluated for their inhibition of AChE, butyrylcholinesterase (BChE), and AChE-induced Aβ aggregation. Compounds **1**−**4** were the most potent inhibitors of the series, which exhibited inhibitory activity against AChE (IC$_{50}$ 1.4−3.1 μM) and, for **1**, Aβ aggregation (77.6%). Molecular docking studies were also performed to investigate interaction of these compounds with the active site of AChE.
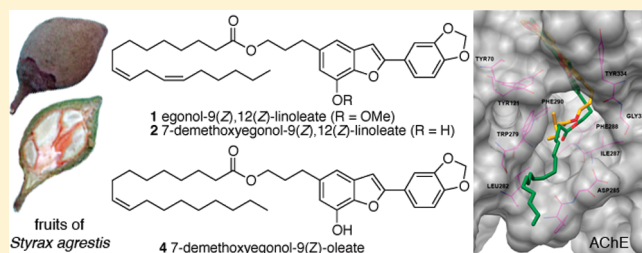
Alzheimer's disease (AD), a progressive neurodegenerative disorder of the central nervous system associated with cognitive and memory loss, is becoming one of the most serious threats to life expectancy for elderly people.[1,2] The main pathological changes in the AD brain include extracellular deposition of beta amyloid (Aβ) in senile plaques, the appearance of intracellular neurofibrillary tangles, and extensive neuronal loss.[3,4] AD is also characterized by a pronounced alteration of the cholinergic neurotransmitter system, a consistent cholinergic deficit, and synaptic changes in the brain resulting in memory impairments.[5] Acetylcholinesterase (AChE) is the key enzyme responsible for the metabolic and catalytic hydrolysis of acetylcholine and promotes the aggregation and deposition of Aβ peptide.[6−8] Aβ deposition leads to neuronal death through oxidative stress, excitotoxicity, energy depletion, inflammation, and apoptosis.[4] One promising therapeutic strategy for AD may consist of concomitantly restoring native ACh levels and reducing the formation of toxic Aβ fibrils.[4,9] Such a strategy may be realized by dual-function molecules possessing the ability to inhibit AChE activity and prevent Aβ peptide aggregation.

In our ongoing efforts to find new AChE inhibitors from natural sources, part of our plant extract library (9327 extracts) was screened by high-throughput assay. In preceding studies we isolated acylphenols from *Myristica crassa* (Myristicaceae) and turrianes from *Kermadecia rotundifolia* (Proteaceae) as new AChE inhibitors.[10,11] We have since found that an EtOAc extract obtained from the fruits of *Styrax agrestis* A. Chev. (Styracaceae)

significantly inhibited AChE activity. *Styrax* is the largest genus of the Styracaceae family, which contains approximately 130 species occurring in tropical and subtropical regions.[12] *Styrax* species have been traditionally used in herbal medicine to treat various diseases.[13] *Styrax* species contain egonol, a natural benzofuran having anticomplement, antifungal, and antibacterial activities.[13−15] A literature survey revealed that no phytochemical study has been carried out on *S. agrestis*. In the present study we report a bioassay-guided isolation and structure elucidation of three new and 10 known egonol-type benzofurans from an EtOAc extract of fruits of *S. agrestis*, as well as their inhibitory activities on AChE, BChE, and AChE-induced Aβ aggregation. Several egonol analogues were also prepared to study structure−activity relationships in this series. The binding mode of some of the molecules to AChE binding sites was also investigated by molecular docking simulations.

■ RESULTS AND DISCUSSION

The EtOAc extract of fruits of *S. agrestis* significantly inhibited recombinant human AChE (*h*AChE) and *Electrophorus electricus* AChE (*Ee*AChE) activity (100% inhibitory effect at 10 μg/mL). The MeOH extract was inactive. One hundred milligrams of the EtOAc extract was filtered on polyamide to remove tannins, and

15 mg of the filtered extract was fractionated on a semipreparative C_{18} column to give nine subfractions according to a standardized method.[16] The AChE bioassay yielded two active subfractions (100% inhibitory effect at 10 μg/mL), which were used as references for further fractionation. The EtOAc extract (3.5 g) was then subjected to silica gel column chromatography (CC), and preparative HPLC led to the isolation of three new (**1**, **2**, and **4**) and 10 known 2-arylbenzofurans (**3**, **5**, **6**−**13**). The known compounds were identified by comparing their physical constants with those reported in the literature: egonol oleate (**3**),[17] egonol-2-methylbutanoate (**5**),[18] 7-demethoxylegonol-2-methylbutanoate (**6**),[18] 7-demethoxylegonol acetate (**7**),[19] egonol propanoate (**8**),[20] egonol-2-methylpropanoate (**9**),[21] egonol butanoate (**10**),[19] egonol acetate (**11**),[22] 7-demethoxyegonol (**12**),[23] and egonol (**13**).[15] To the best of our knowledge, **3** has not been described before as a natural compound but has been obtained by semisynthesis from egonol.[17] 7-Demethoxyegonol (**12**) and egonol (**13**) were also obtained after alkaline hydrolysis of the EtOAc extract.

Compound **1** was a pale yellow oil, and its sodiated molecular formula was determined to be $C_{37}H_{48}O_6Na$ by HRESIMS. The ^{13}C NMR signals of the alcohol part of compound **1** were superimposable to those of **13**, while the ^{13}C NMR signals of the unsaturated fatty acid moiety were similar to those of linoleic acid.[24] The ^1H NMR and ^{13}C NMR spectra, HSQC, and HMBC of **1** showed signals assignable to a *cis,cis*-1,4-pentadiene unit of a long-chain unsaturated fatty acid moiety.[25] Comparison of the ^{13}C NMR data of **1** with those of **13** indicated an esterification shift at the C-3″ position of **1**, and a long-range correlation was observed between H-3″ and C-1‴ in the HMBC spectra. Ozonolysis of **1** gave aldehyde **14**. This indicated that the *cis,cis*-1,4-pentadiene unit was at C-9‴ of the unsaturated fatty acid. Alkaline hydrolysis of **1** with 10% NaOH−EtOH yielded linoleic acid and **13**. Compound **1** was thus assigned the structure egonol-9(Z),12(Z)-linoleate.
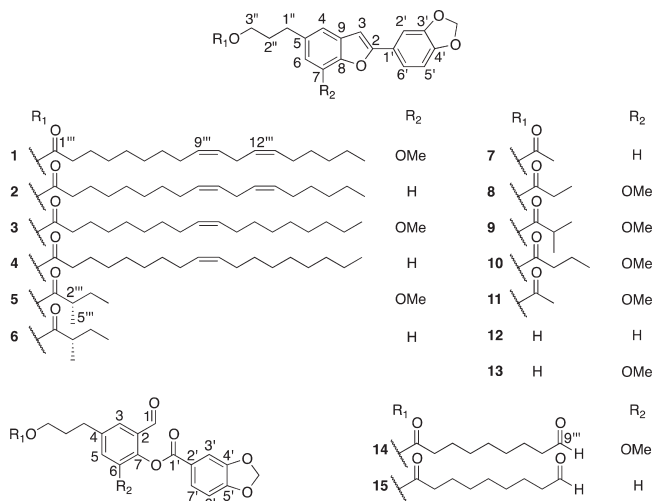
Compound **2** gave a sodiated molecular formula of $C_{36}H_{46}O_5Na$ (HRESIMS). The ^{13}C NMR signals of the 2-arylbenzofuran part were superimposable with those of **12**, and the signals of the fatty acid moiety were similar to those of linoleic acid. Ozonolysis of **2** yielded aldehyde **15**, and alkaline hydrolysis of **2** with 10% NaOH−EtOH liberated linoleic acid and **12**. Thus, **2** was determined to be 7-demethoxyegonol-9(Z),12(Z)-linoleate.

The sodiated molecular formula of compound **4** ($C_{36}H_{48}O_5Na$) was deduced from HRESIMS measurements, and the ^1H and ^{13}C NMR spectra of **4** were similar to those of **2**. The carbon signals of the alcohol moiety were nearly superimposable with those of **12**, while the signals of the fatty acid moiety were similar to those of oleic acid.[26] Comparison of the ^{13}C NMR data of **4** with those of **12** indicated an esterification shift at C-3″, and the HMBC experiment exhibited a long-range correlation between H-3″ and C-1‴. Alkaline hydrolysis of **4** yielded oleic acid and **12**, and ozonolysis of **4** yielded aldehyde **15**. Consequently, compound **4** was characterized as 7-demethoxyegonol-9(Z)-oleate.

The HRESIMS of compound **5** revealed a sodiated molecular formula of $C_{24}H_{26}O_6Na$. Examination of the 1D and 2D NMR spectra suggested that **5** was egonol-2‴-methyl butanoate, previously isolated from *Styrax obassia*.[18] As the C-2 configuration was unknown, the (S)-2‴-methyl butyrate ester was prepared from egonol (Figure 1). Spectral and analytical data were similar to those of **5**, and the sign of optical rotation of the synthesized compound and of **5** was the same. Thus, the absolute configuration of compound **5** was deduced as S at C-2‴.

Compound **6** was obtained as an optically active oil, and the HRESIMS indicated a sodiated molecular formula of $C_{23}H_{24}O_5Na$. Examination of the 1D and 2D NMR spectra suggested that **6** was 7-demethoxylegonol-2-methylbutanoate, previously isolated from *S. obassia*.[18] The positive sign of the optical rotation for **6** was the same as that of **5**, suggesting the S absolute configuration at C-2‴.

In order to examine structure−activity relationships in this benzofuran series, other derivatives were prepared from **13**. The synthetic pathway employed for the preparation of egonol derivatives is outlined in Figure 1.

Compound **16** was obtained by oxidation of **13** using Dess-Martin periodinane in CH_2Cl_2. The ^1H and ^{13}C NMR spectra of **16** showed an aldehyde proton signal at δ_H 9.74 (H-3″) corresponding to the carbon signal at δ_C 202.9 (C-3″) instead of signals for a primary alcohol as in egonol. The structure of **16** was established as 3-[2-(1,3-benzodioxol-5-yl)-7-methoxy-1-benzofuran-5-yl]propanal.[17]

Compound **17** was prepared from **13** by oxidation using CrO_3 in CH_2Cl_2−pyridine. The main differences in the ^1H and ^{13}C NMR spectra of **17** and **16** were the absence of signals at δ_H 9.74 (H-3″ in **16**) and δ_C 202.9 (C-3″ in **16**) and the presence of a signal at δ_C 177.0, which confirmed the carboxylic function. Therefore, **17** was established as the known 3-[2-(1,3-benzodioxol-5-yl)-7-methoxy-1-benzofuran-5-yl]propionic acid (egonoic acid).[27]

Compound **18** was obtained from the reaction of **13** with *tert*-butyl isocyanate in dry CH_3CN and gave an ion peak at m/z 448.1733 $[M + Na]^+$ ($C_{24}H_{27}NO_6Na$). The ^1H NMR spectrum of **18** showed that the resonance of H-3″ was shifted downfield compared to that of egonol. The ^{13}C NMR spectrum displayed 24 carbons signals. A HMBC correlation was observed between the C-1‴ carbonyl of a carbamate group and H-3″ in the egonol moiety. Thus, compound **18** was identified as N-*tert*-butyl egonolcarbamate.

Compound **19** was prepared by treatment of **13** with phenyl isocyanate in dry CH_3CN. The ^1H NMR spectrum of **19** showed that the resonance of H-3″ was also shifted downfield compared to that of egonol. The ^{13}C NMR spectrum of **19** exhibited 26 carbon signals, and a HMBC correlation was observed between the carbonyl carbon C-1‴ of the carbamate
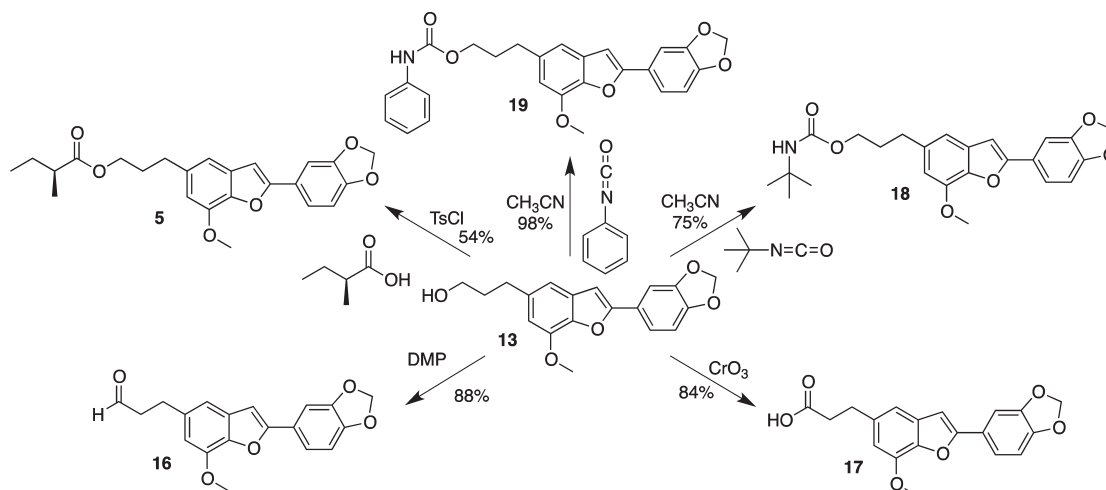
Figure 1. Preparation of egonol derivatives.

Table 1. Inhibition of *Ee*AChE and *h*AChE by Benzofuran Derivatives[a,b]

compound	*Ee*AChE	*h*AChE
1	1.4 ± 0.3	1.7 ± 0.2
2	2.0 ± 0.9	2.7 ± 0.4
3	1.4 ± 0.5	1.8 ± 0.3
4	2.2 ± 0.8	3.1 ± 0.6
5	4.8 ± 0.6	5.9 ± 0.7
6	5.5 ± 0.7	6.1 ± 0.8
9 + 10	3.6 ± 0.6	5.2 ± 0.5
19	3.3 ± 0.6	4.5 ± 0.6
tacrine[c]	50 ± 3 nM	1026 ± 72 nM

[a] Results are expressed as means of IC_{50} values (the concentration that inhibits AChE by 50%) in μM, and data were obtained from duplicate experiments. [b] For the enzymes used, see Experimental Section. [c] Tacrine was used as reference.

Table 2. Inhibition of AChE-Induced Aβ Aggregation by Benzofuran Derivatives

compound	inhibition (%) at 100 μM
1	77.6
5	70.5
11	64.6
13	61.6
19	86.5
propidium	54.1

AChE. None of the compounds (**1**−**19**) inhibited BChE activity ($IC_{50} > 20 \, \mu$M).

Five compounds (**1**, **5**, **11**, **13**, and **19**) were selected to evaluate their ability to inhibit AChE-induced Aβ aggregation using a thioflavin T fluorimetric assay.[29] Aβ_{1-40} (230 μM) was incubated at 25 °C for 48 h with AChE (2.3 μM) in the presence of test compounds at 100 μM, and propidium iodine was used as a reference. The Aβ aggregation inhibitory potency of the compounds is reported in Table 2. Compound **1**, a selective AChE inhibitor, significantly inhibited AChE-induced Aβ aggregation by 77.6%. Compounds **11** and **13** did not show any AChE inhibition, whereas their aggregation inhibitory potency was 64.6% and 61.6%, respectively, at 100 μM concentrations. These data suggest that the inhibitory effect of benzofurans on Aβ aggregation is probably independent of AChE inhibition and may be associated with their direct binding to Aβ peptide. In accordance with our results, Howlett et al. revealed that the benzofuran analogue SKF-64346 prevented aggregation by a process involving binding of the benzofuran to Aβ peptide, suggesting that a specific recognition site might exist for benzofurans on Aβ peptide.[30] These findings are also consistent with the observations that benzofuran-based hybrid compounds significantly inhibited AChE/BChE activities and exhibited significant inhibition of Aβ aggregation.[31]

Molecular modeling studies were performed in order to investigate how these compounds might interact with the active site of AChE. During the last two decades, a large number of molecular modeling studies focused on AChE have been published using different approaches (pharmacophore-based virtual
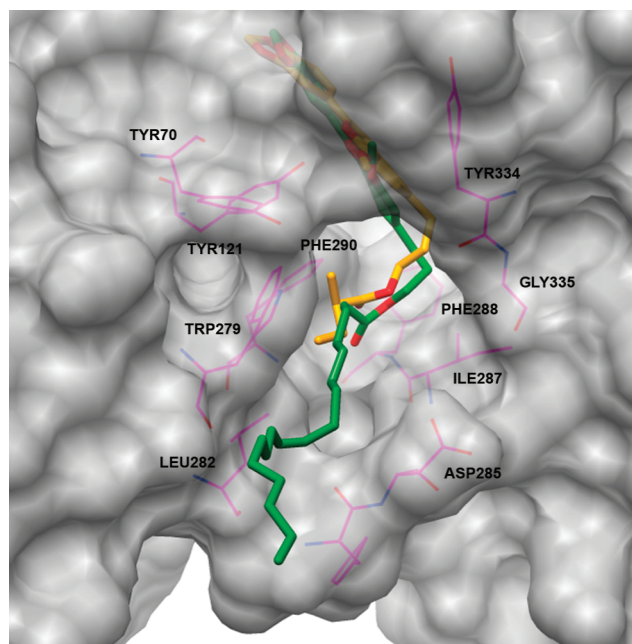
group and H-3″. Thus, compound **19** was identified as *N*-phenyl egonolcarbamate.

The inhibitory potency and selectivity of benzofurans **1**−**19** were evaluated on *Ee*AChE, *h*AChE, and BChE by a modified Ellman's colorimetric method.[28] The IC_{50} values of active compounds are compared in Table 1. The egonol esters **1**−**6**, **9 + 10**, and **19** significantly inhibited both *Ee*AChE and *h*AChE activity, whereas **7**, **8**, **11**−**13**, **16**, and **17** were inactive. The data indicate that the degree of inhibition of AChE is related to the length and bulkiness of the alkyl ester group. Alkyl chains with more than three carbon units led to compounds with anticholinesterase activity. Nevertheless, further increase in chain length did not significantly enhance AChE inhibition, as illustrated by the close IC_{50} values of **1** and **3** compared to **5** or **2** and **4** compared to **6**. In addition, it was found that a methoxy group at C-7 had no effect on activity since the linoleate and oleate esters of egonol (**1** and **3**, respectively) have IC_{50} values very close to their 7-demethoxylate analogues (**2** and **4**). Furthermore, oxidation and conversion of the double bond of the furan ring of **1**−**4** into the corresponding aldehyde-ester derivatives (**14** and **15**) resulted in loss of anti-AChE activity. Thus, both the furan and ester groups play important roles in the inhibition of

Figure 2. Superposition of **3** (green) and **5** (yellow) in the binding site of acetylcholinesterase, at the termination of the molecular dynamics simulation (10 ns). Hydrophobic residues at the peripheral site involved in ligand stabilization are shown in magenta. This mode of binding is representative for compounds **1**−**5** isolated from *S. agrestis*.

screening, different types of molecular docking and structure-based virtual screening, molecular dynamics) or a combination of these (see Supporting Information for references). All of these studies involved AChE inhibitors having at least one positively charged nitrogen atom or a nitrogen-containing polar group, which generally drives the overall binding mode in the AChE site. Several nitrogen-free AChE inhibitors have been reported recently, mainly isolated from natural sources.[32] Three-dimensional structures of compounds **1**−**7** and **11**−**13** were built and used for molecular docking in the binding site of AChE. In agreement with the experimental data for anticholinesterase activity, only compounds **1**−**6** could be successfully docked, and the resulting ligand conformations showed interactions with both catalytic and peripheral sites, the more rigid cyclic system being positioned inside the catalytic site of the protein (Figure 2). During the docking process, the ligands were fully flexible and the protein was rigid, the binding site being defined as a sphere with a radius of 20 Å around the OH group of SER200. For compounds presenting ambiguity in the assignment of a chiral atom configuration (e.g., **6**), both stereoisomers were considered.

Using the docking results as starting conformations, molecular dynamics simulations were carried out over 10 ns in order to introduce protein flexibility and to evaluate the possibility of an induced fit that could take place upon ligand binding. In most cases a slight rearrangement of the ligand in the binding site was observed, concomitant with some changes in the protein side-chain conformations in order to accommodate the presence of the ligand. Root-mean-square deviation (rmsd) values of 2.5 Å were typically obtained for the protein. For the ligand, the rmsd values were more variable, with an important contribution from the movement of the long aliphatic chains in the case of **1**−**4** (see Supporting Information). Very few protein−ligand hydrogen bonds were identified, the interactions being mainly hydrophobic.

Among these, three main hydrogen bonds were evident during the molecular dynamics simulations, which anchor the ligand in the AChE binding site: the carbonyl O atom from the ligand ester group interacts with the backbone NH from Phe288 and O atoms from the ligand 1,2-(methylenedioxy)benzene group interact with the backbone NH from Ser124 and OH group from Tyr130. Particularly interesting are the hydrophobic residues situated at the peripheral site (Figure 2), which are involved in ligand stabilization. These interactions are essential for AChE inhibition since **7** and **11**−**13**, which do not contain a reasonably voluminous hydrophobic ester substituent, are not active. However, very long aliphatic chains do not increase the inhibitory activity, as the terminal atoms fall outside the binding site. Finally the methoxy substituent of the benzofuran moiety does not seem to be essential for inhibition, this substituent making only limited hydrophobic contacts with Asp72 and Tyr334.

In conclusion, we have identified a novel series of benzofuran AChE inhibitors with significant inhibitory effects on Aβ aggregation. The structure−activity relationships suggest that the furan ring, the ester group, and the length of the hydrocarbon side chain are the key structural features contributing to the inhibitory potency of the benzofuran derivatives against AChE. Molecular modeling calculations propose a binding mode for this class of compounds on AChE and have identified several residues at the peripheral site that are important for the inhibitory effect. Our data suggest that these benzofuran derivative dual-function molecules are capable not only of inhibiting AChE activity but also of preventing Aβ aggregation and provide a chemical template for further optimization.

■ EXPERIMENTAL SECTION

General Experimental Procedures. Optical rotations were recorded in CH_2Cl_2 at 25 °C with a Perkin-Elmer 341 polarimeter. IR spectra were recorded on a Nicolet FT-IR 205 spectrophotometer. UV spectra were recorded on a Varian Cary 100 UV−visible spectrophotometer. ^1H and ^{13}C spectra were recorded in $CDCl_3$ on an Avance 300 Bruker spectrometer operating at 300.17 and 75.48 MHz, respectively, or on an Avance 500 Bruker (^1H, 500.13; ^{13}C, 125.77 MHz). ^1H chemical shifts were referenced relative to $CDCl_3$ at 7.24 ppm and ^{13}C chemical shifts to the central peak of $CDCl_3$ at 77.23 ppm. High-resolution mass spectra (HRMS) were recorded with either a MALDI-TOF mass spectrometer (Voyager-De STR; Perspective Biosystems) or an ESI-TOF mass spectrometer (LCT Premier; Waters). TLC was performed on Si gel 60 F$_{254}$. Column chromatography was carried out on Merck Si gel 60. Analytical and preparative HPLC were performed on a Waters autopurification HPLC system (Waters 2525) using a Kromasil C_{18} column (250 × 4.5 mm i.d. for analytical and a 250 × 21.2 mm i.d. column for preparative, stainless steel, 5 μm Thermo). The gradient mobile phase was MeCN−H_2O (3:1) to 100% MeCN. The flow rate was 17 mL/min, and the elution was monitored with a UV−vis diode array detector (190−600 nm, Waters 2996) and a PL-ELS 1000 ELSD Polymer Laboratory detector. CombiFlash Companion chromatography (CCC) was carried out on silica gel colums (Redisep 4 g).

Plant Material. Ripe fruits of *S. agrestis* were collected in Vietnam by D. D. Cuong (Institute of Chemistry, VAST, Hanoi) in May 2005 at Thua Thien, Hue district, and identified by Q. B. Nguyen from the Institute of Botany, VAST, Hanoi, where a voucher specimen VN-1512 is deposited.

Extraction and Isolation. Dried, powdered fruits of *S. agrestis* (1060 g) were extracted with EtOAc (250 mL × 3) and MeOH (250 mL × 3) at 40 °C. The filtrates were evaporated under vacuum to give the EtOAc (26.5 g) and MeOH (100.4 g) extracts. These extracts were evaluated using the AChE assay. The MeOH extract had no activity

at 10 μg/mL. The EtOAc extract exhibited 100% inhibition at 10 μg/mL. A 100 mg aliquot of the crude EtOAC extract was dissolved in a 1:1 mixture of EtOAc−MeOH and filtered on a polyamide cartridge. The filtered extract was then fractionated on a semipreparative C_{18} column, according to a previous method.[16] Subfractions 6 and 7 (Fr.6, Fr.7) gave 100% inhibition of AChE activity at 10 mg/mL and were used as positive references. The EtOAc extract (3.5 g) was then subjected to silica gel CCC eluted with a heptane−EtOAc−MeOH gradient. Fractions 3, 4, and 5 (Fr.3−5) of the EtOAc extract were the most active. Fr.3 (165.8 mg) was further separated by CC on a Sunfire RP-18 column (290 × 150 mm i.d., Waters) using MeCN. Four compounds were obtained: **1** (7.4 mg), **2** (5.0 mg), **3** (11.9 mg), and **4** (4.1 mg). Fr.4 (126.2 mg) was further separated by HPLC (H_2O−MeCN, 5:95) to give compounds **5** (31.0 mg) and **6** (6.8 mg). Fr.5 (155.6 mg) was subjected to RP-HPLC eluted with H_2O−MeCN (10:90) at 17 mL/min to yield compounds **7** (2.3 mg), **8** (1.3 mg), a 66:44 mixture of **9** and **10** (8.1 mg), **11** (7.1 mg), **12** (12.4 mg), and **13** (276 mg).

Compound 1: oil; UV (CH_2Cl_2) λ_{max} (log ε) 211 (4.03), 228 (4.21), 318 (4.23) nm; IR (CH_2Cl_2) ν_{max} 2925, 1731, 1600, 1475, 1366, 1232, 1146, 1040, 930 cm^{-1}; ^{1}H NMR (CDCl$_3$, 300 MHz) δ 7.38 (1H, dd, J = 8.2, 1.7 Hz, H-6′), 7.30 (1H, d, J = 1.7 Hz, H-2′), 6.93 (1H, d, J = 1.3 Hz, H-4), 6.85 (1H, d, J = 8.2 Hz, H-5′), 6.77 (1H, s, H-3), 6.58 (1H, d, J = 1.3 Hz, H-6), 5.99 (2H, s, OCH_2O), 5.36 (1H, dt, J = 10.7, 7.0 Hz, H-12‴), 5.34 (1H, dt, J = 10.8, 7.0 Hz, H-10‴), 5.32 (1H, dt, J = 10.8, 7.1 Hz, H-9‴), 5.30 (1H, dt, J = 10.7, 7.0 Hz, H-13‴), 4.10 (2H, t, J = 6.5 Hz, H-3″), 4.01 (3H, s, OCH_3), 2.75 (2H, brt, J = 5.8 Hz, H-11″), 2.73 (2H, brt, J = 7.5 Hz, H-1″), 2.29 (2H, t, J = 7.5 Hz, H-2‴), 2.03 (2H, dd, J = 8.7, 6.4 Hz, H-8″), 2.03 (2H, dd, J = 13.1, 6.6 Hz, H-8‴), 1.98 (2H, dd, J = 7.5, 6.5 Hz, H-2″), 1.61 (2H, m, H-3‴), 1.30 (14H, m, H-4‴-H-7‴, H-15‴-H-17‴), 0.87 (3H, t, J = 6.8 Hz, H-18‴); ^{13}C NMR data (CDCl$_3$, 75 MHz) δ 174.1 (C, C-1‴), 156.4 (C, C-2), 148.3 (C, C-3′), 148.2 (C, C-4′), 145.0 (C, C-7), 142.8 (C, C-8), 137.2 (C, C-5), 131.3 (C, C-9), 130.4 (CH, C-13‴), 130.2 (CH, C-9‴), 128.3(CH, C-12‴), 128.1 (CH, C-10‴), 124.9 (C, C-1′), 119.4 (CH, C-6′), 112.6 (CH, C-4), 108.8 (CH, C-5′), 107.7 (CH, C-6), 105.8 (CH, C-2′), 101.3 (CH$_2$, OCH_2O), 100.6 (CH, C-3), 63.8 (CH$_2$, C-3″), 56.4 (CH$_3$, OCH_3), 34.6 (CH$_2$, C-2‴), 32.8 (CH$_2$, C-1″), 31.7 (CH$_2$, C-16‴), 31.0 (CH$_2$, C-2″), 29.8 (CH$_2$, C-7‴), 29.6 (CH$_2$, C-6‴), 29.4 (CH$_2$, C5‴), 29.4 (CH$_2$, C-15‴), 29.3 (CH$_2$, C-4‴), 27.4 (CH$_2$,C-8″), 27.4 (CH$_2$, C-14‴), 25.8 (CH$_2$, C-11‴), 22.8 (CH$_2$, C-17‴), 14.3 (CH$_3$, C-18‴); MALDI-TOF-HRMS m/z 611.3359 [M + Na]$^+$ (calcd for C$_{37}$H$_{48}$O$_6$Na, 611.3349).

Compound 2: oil; UV (CH_2Cl_2) λ_{max} (log ε) 228 (4.04), 320 (4.23) nm; IR (CH_2Cl_2) ν_{max} 2925, 2854, 1731, 1503, 1488, 1472, 1234, 1175, 1039, 931 cm^{-1}; ^{1}H NMR (CDCl$_3$, 500 MHz) δ 7.37 (1H, d, J = 8.4 Hz, H-7), 7.36 (1H, dd, J = 8.2, 1.4 Hz, H-6′), 7.32 (1H, brs, H-4), 7.28 (1H, d, J = 1.4 Hz, H-2′), 7.05 (1H, dd, J = 8.4, 1.3 Hz, H-6), 6.86 (1H, d, J = 8.2 Hz, H-5′), 6.79 (H, s, H-3), 5.99 (2H, s, OCH_2O), 5.37 (1H, dd, J = 10.8, 5.2 Hz, H-12‴), 5.34 (1H, dd, J = 10.8, 7.4 Hz, H-10‴), 5.32 (1H, dd, J = 10.8, 8.0 Hz, H-9‴), 5.30 (1H, dd, J = 10.1, 7.0 Hz, H-13‴), 4.09 (2H, t, J = 6.5 Hz, H-3″), 2.75 (2H, d, J = 6.4 Hz, H-11″), 2.75 (2H, t, J = 7.6 HZ, H-1″), 2.28 (H, t, J = 7.5 Hz, H-2‴), 2.03 (2H, dd, J = 13.7, 6.8 Hz, H-14‴), 1.99 (2H, dd, J = 9.7, 6.4 Hz, H-8‴), 1.96 (2H, dd, J = 7.5, 6.5 Hz, H-2″), 1.61 (2H, m, H-3‴), 1.30 (14H, m, H-4‴-H-7‴, H-15‴-H-17‴), 0.87 (3H, t, J = 6.7 Hz H-18‴); ^{13}C NMR data (CDCl$_3$, 125 MHz) δ 174.1 (C, C-1‴), 156.3 (C, C-2), 153.6 (C, C-8), 148.3 (C, C-3′), 148.2 (C, C-4′), 136.1 (C, C-5), 130.5 (CH, C-13‴), 130.3 (CH, C-9‴), 129.8 (C, C-9), 128.3 (CH, C-12‴), 128.1 (CH, C-10‴), 125.1 (C, C-1′), 124.7 (C, C-6), 120.3 (CH, C-4), 119.3 (CH, C-6′), 111.0 (CH, C-7), 108.9 (CH, C-5′), 105.7 (CH, C-2′), 101.5 (CH$_2$, OCH_2O), 100.2 (CH, C-3), 63.8 (CH$_2$, C-3″), 34.6 (CH$_2$, C-2‴), 32.4 (CH$_2$, C-1″), 31.8 (CH$_2$, C-16‴), 31.1 (CH$_2$, C-2″), 29.8 (CH$_2$, C-7‴), 29.6 (CH$_2$,C-6‴), 29.4 (CH$_2$,C-4‴), 29.4 (CH$_2$,C-5‴), 29.4 (CH$_2$,C-15‴), 27.4 (CH$_2$, C-8″), 27.4 (CH$_2$, C-14‴), 25.8 (CH$_2$, C-11‴), 25.2 (CH$_2$, C-3‴), 22.8 (CH$_2$, C-17‴), 14.3 (CH$_3$,

C-18‴); MALDI-TOF-HRESIMS m/z 581.3284 [M + Na]$^+$ (calcd for C$_{36}$H$_{46}$O$_5$Na, 581.3243).

Compound 3: oil; UV (CH_2Cl_2) λ_{max} (log ε) 210 (4.16), 229 (4.04), 319 (4.23) nm; IR (CH_2Cl_2) ν_{max} 2922, 2851, 1734, 1600, 1503, 1475, 1364, 1232, 1146, 1039, 930 cm^{-1}; ^{1}H and ^{13}C NMR spectra, see Ozturk et al.;[17] HRESIMS m/z 613.3506 [M + Na]$^+$ (calcd for C$_{37}$H$_{50}$O$_6$Na, 613.3505).

Compound 4: oil; UV (CH_2Cl_2) λ_{max} (log ε) 210 (4.14), 229 (4.05), 319 (4.23) nm; IR (CH_2Cl_2) ν_{max} 2923, 1732, 1600, 1503, 1467, 1364, 1233, 1146, 1039, 930 cm^{-1}; ^{1}H NMR (CDCl$_3$, 500 MHz) δ 7.37 (1H, d, J = 8.4 Hz, H-7), 7.36 (1H, dd, J = 8.2, 1.4 Hz, H-6′), 7.32 (1H, d, J = 1.3 Hz, H-4), 7.28 (1H, d, J = 1.4 Hz, H-2′), 7.05 (1H, brd, J = 8.4 Hz, H-6), 6.86 (1H, d, J = 8.2 Hz, H-5′), 6.79 (H, s, H-3), 5.99 (2H, s, OCH_2O), 5.32 (1H, ddt, J = 11.1, 10.7, 6.0 Hz, H-9‴), 5.32 (1H, dd, J = 11.1, 5.9 Hz, H-10‴), 4.09 (2H, t, J = 6.5 Hz, H-3″), 2.75 (2H, t, J = 7.6 HZ, H-1″), 2.28 (H, t, J = 7.5 Hz, H-2‴), 1.98 (2H, m, H-8‴), 1.98 (2H, m, H-11‴), 1.98 (2H, m, H-2″), 1.60 (2H, m, H-3‴), 1.29 (20H, m, H4‴-H-7‴, H-12‴−H-17‴), 0.86 (3H; t, J = 6.7 Hz, H-18‴); ^{13}C NMR data (CDCl$_3$, 125 MHz) δ 174.1 (C, C-1‴), 156.3 (C, C-2), 153.6 (C, C-8), 148.3 (C, C-3′), 148.2 (C, C-4′), 136.1 (C, C-5), 130.2 (CH, C-9‴), 129.9 (CH, C-10‴), 129.8 (C, C-9), 125.1 (C, C-1′), 124.8 (C, C-6), 120.2 (CH, C-4), 119.3 (CH, C-6′), 111.0 (CH, C-7), 108.9 (CH, C-5′), 105.7 (CH, C-2′), 101.5 (CH2, OCH_2O), 100.2 (CH, C-3), 63.8 (CH$_2$, C-3″), 34.6 (CH$_2$, C-2‴), 32.4 (CH$_2$, C-1″), 31.1 (CH$_2$, C-2″), 29.9 (CH$_2$, C-7‴), 29.9 (CH$_2$, C-12‴), 29.7 (CH$_2$, C-6‴), 29.5 (CH$_2$, C-5‴), 29.5 (CH$_2$, C-13‴), 29.5 (CH$_2$, C-14‴), 29.4 (CH$_2$, C-4‴), 29.4 (CH$_2$, C-15‴), 27.4 (CH$_2$,C-8‴), 27.4 (CH$_2$, C-11‴), 25.2 (CH$_2$, C-3‴), 22.9 (CH$_2$, C-17‴), 14.3 (CH$_3$, C-18‴); MALDI-TOF-HRE-SIMS m/z 583.3436 [M + Na]$^+$ (calcd for C$_{36}$H$_{48}$O$_5$Na, 583.3399).

Compound 5: oil; $[\alpha]^{25}_D$ +5.2 (c 1.0, CH_2Cl_2); UV (CH_2Cl_2) λ_{max} (log ε) 211 (4.05), 228 (4.09), 318 (4.22) nm; IR (CH_2Cl_2) ν_{max} 2922, 1729, 1600, 1475, 1365, 1231, 1146, 1040, 930 cm^{-1}; ^{1}H and ^{13}C spectra of **5**, see Takanashi et al.;[18] MALDI-TOF-HRESIMS, m/z 433.1682 [M + Na]$^+$ (calcd for C$_{24}$H$_{26}$O$_6$Na, 433.1627).

Synthesis of Compound 5. To a stirred solution of **13** (20.0 mg, 0.061 mmol) in pyridine (0.5 mL) were added (S)-(+)-2-methylbutyric acid (12.5 mg, 0.061 mmol) and p-toluenesulfonyl chloride (2.2 mg, 0.003 mmol) in CH_2Cl_2 (1 mL). The reaction mixture was refluxed for 8 h and stirred for a further 72 h at rt. The reaction mixture was diluted with H_2O (10 mL) and extracted with CH_2Cl_2 (15 mL × 3). The combined organic layers were dried over anhydrous Na$_2$SO$_4$, filtered through Celite, and evaporated to dryness. The residue was purified by CCC (heptane−EtOAc, 4:1) to afford a product identical to isolated compound **5** (13.4 mg, 54%); $[\alpha]^{25}_D$ +4.4 (c 1.0, CH_2Cl_2).

Compound 6: oil; $[\alpha]^{25}_D$ +8.5 (c 0.5, CH_2Cl_2). UV (CH_2Cl_2) λ_{max} (log ε) 228 (3.93), 320 (4.23) nm; IR (CH_2Cl_2) ν_{max} 2926, 1727, 1613, 1503, 1488, 1446, 1468, 1360, 1231, 1182, 1149, 1037, 930 cm^{-1}; ^{1}H and ^{13}C spectra, see Takanashi et al.;[18] HRESIMS m/z 403.1566 [M + Na]$^+$ (calcd for C$_{23}$H$_{24}$O$_5$Na, 403.1580).

Alkaline Hydrolysis. The crude EtOAc extract (16.5 g) of *S. agrestis* was hydrolyzed with 15% NaOH in 50% EtOH at 100 °C for 4 h under argon. The reaction mixture was cooled to rt. The resulting suspension, after removal of alcoholic solvent under reduced pressure, was diluted with H_2O (500 mL) and then extracted with CH_2Cl_2 (150 mL × 3). The combined organic layers were dried over anhydrous Na$_2$SO$_4$, filtered trough Celite, and evaporated to give the crude hydrolysate (5.9 g). The latter was purified by CCC (heptane−EtOAc; linear gradient from 1:0 to 1:1) to afford **12** (58.6 mg, demethoxyegonol[23]) and **13** (947.3 mg, egonol[15]).

Ozonolysis of Compounds 1, 2, 3, and 4. Ozonolysis[33] was carried out in a long-necked, 50 mL standard flask equipped with a magnetic stirring bar and with an insert containing a dropping funnel and a gas inlet tube that reached the bottom of the reactor. A solution of **1**−**4** (3−5 mg each) in CH_2Cl_2−MeOH (1:1, 5 mL) was added to the

reactor, which was cooled to −78 °C with a dry ice−acetone bath. The reactor content was mixed with a slow stream of argon. Ozone was generated and passed through the mixture. Excess ozone was removed by flushing the reactor with argon. Dimethyl sulfide (0.5 mL) was added, and the mixture was stirred for 12 h at rt. The volatile components were removed on a rotary evaporator. Ozonolysis of **1** and **3** yielded aldehyde **14**, and ozonolysis of **2** and **4** gave aldehyde **15**.

Compound **14**: oil; ^{1}H NMR (CDCl$_3$, 500 MHz) δ 10,14 (1H, s, H-1), 9.74 (1H, t, *J* = 1.5 Hz, H-9′′′), 7.84 (1H, dd, *J* = 8.2, 1.7 Hz, H-7′), 7.61 (1H, d, *J* = 1.7 Hz, H-3′), 7.32 (1H, d, *J* = 1.8 Hz, H-3), 7.04 (1H, d, *J* = 1.6 Hz, H-5), 6.91 (1H, d, *J* = 8.2 Hz, H-6′), 6.07 (2H, s, OCH$_2$O), 4.11 (2H, brt, *J* = 6.4 Hz, H-3′′), 3.82 (3H, s, OCH$_3$), 2.73 (2H, dd, *J* = 9.0, 6.7 Hz, H-1′′), 2.40 (2H, td, *J* = 7.3, 1.7 Hz, H-8′′′), 2.30 (2H, t *J* = 7.5 Hz, H-2′′′), 1.98 (2H, dd, *J* = 9.0, 6.4 Hz H-2′′), 1.60 (2H, m, H-3′′′), 1.60 (2H, m, H-7′′′), 1.30 (2H, m, H-4′′′), 1.30 (2H, m, H-5′′′), 1.30 (2H, m, H-6′′′); ^{13}C NMR data (CDCl$_3$, 125 MHz) δ 202.9 (C, C-9′′′), 189.2 (CH, C-1), 174.1 (C, C-1′′′), 164.3 (C, C-1′), 152.9 (C, C-5′), 152.0 (C, C-4′), 129.3 (C, C-2), 126.9 (CH, C-7′), 124.9 (C, C-2′), 119.8 (CH, C-3), 118.3 (CH, C-5), 110.4 (CH, C-3′), 108.5 (CH, C-6′), 102.5 (CH$_2$, OCH$_2$O), 63.6 (CH$_2$, C-3′′), 56.6 (CH$_3$, OCH$_3$), 44.5 (CH$_2$, C-8′′′), 34.7 (CH$_2$, C-2′′′), 32.4 (CH$_2$, C-1′′), 30.3 (CH$_2$, C-2′′), 29.3 (CH$_2$, C-6′′′), 29.2 (CH$_2$, C-5′′′), 29.2 (CH$_2$, C-4′′′), 28.4 (CH$_2$, C-7′′′), 25.1 (CH$_2$, C-3′′′); MALDI-TOF-MS 519.23 [M + Li]$^+$, 535.22 [M + Na]$^+$; MALDI-TOF-HRMS *m/z* 535.1938 [M + Na]$^+$ (calcd for C$_{28}$H$_{32}$O$_9$Na, 535.1944).

Compound **15**: oil; ^{1}H NMR (CDCl$_3$, 500 MHz) δ 10,16 (1H, s, H-1), 9.74 (1H, t, *J* = 1.8 Hz, H-9′′′), 7.83 (1H, dd, *J* = 8.2, 1.7 Hz, H-7′), 7.74, (1H, d, *J* = 2.0 Hz, H-3), 7.60 (1H, d, *J* = 1.7 Hz, H-3′), 7.47 (1H, dd, *J* = 8.2, 2.0 Hz, H-5), 7.21 (1H, d, *J* = 8.2 Hz, H-6), 6.91 (1H, d, *J* = 8.2 Hz, H-6′), 6.08 (2H, s, OCH$_2$O), 4.10 (2H, brt, *J* = 6.4 Hz, H-3′′), 2.75 (2H, brt, *J* = 7.9 Hz, H-1′′), 2.40 (2H, td, *J* = 7.3, 1.7 Hz, H-8′′′), 2.29 (2H, t *J* = 7.5 Hz, H-2′′′), 1.98 (2H, dd, *J* = 7.9, 6.4 Hz, H-2′′), 1.61 (2H, m, H-3′′′), 1.61 (2H, m, H-7′′′), 1.32 (2H, m, H-4′′′), 1.32 (2H, m Hz H-5′′′), 1.32 (2H, m, H-6′′′); ^{13}C NMR data (CDCl$_3$, 125 MHz) δ 202.9 (C, C-9′′′), 188.9 (CH, C-1), 173.8 (C, C-1′′′), 164.7 (C, C-1′), 152.8 (C, C-5′), 148.2 (C, C-4′), 139.8 (C, C-4), 135.5 (CH, C-5), 135.2 (C, C-7), 129.5 (CH, C-3), 129.3 (C, C-2), 126.8 (CH, C-7′), 123.8 (CH, C-6), 122.7 (C, C-2′), 110.1 (CH, C-3′), 108.5 (CH, C-6′), 102.2 (CH$_2$, OCH$_2$O), 63.5 (CH$_2$, C-3′′), 43.9 (CH$_2$, C-8′′′), 34.3 (CH$_2$, C-2′′′), 31.6 (CH$_2$, C-1′′), 30.1 (CH$_2$, C-2′′), 28.9 (CH$_2$, C-4′′′), 28.9 (CH$_2$, C-5′′′), 28,9 (CH$_2$, C-6′′′), 24.9 (CH$_2$, C-3′′′), 22.9 (CH$_2$, C-7′′′); MALDI-TOF-MS 489.21 [M + Li]$^+$, 505.18 [M + Na]$^+$; MALDI-TOF-HRMS *m/z* 505.1833 [M + Na]$^+$ (calcd for C$_{27}$H$_{30}$O$_8$Na, 505.1838).

Preparation of 16. Dess-Martin periodinane (79.6 mg, 0.19 mmol) was added to a solution of **13** (61.2 mg, 0.19 mmol) in CH$_2$Cl$_2$ (2 mL), and the mixture was stirred at rt for 12 h. The reaction mixture was washed successively with water (50 mL × 3) and brine (50 mL × 2), dried over anhydrous Na$_2$SO$_4$, and filtered, and the solvent was evaporated in vacuo. The residue was purified by PTLC using heptane−EtOAc (1:1) to give **16**[17] (54.7 mg, 88%).

Preparation of 17. Chromium trioxide (500 mg, 5.0 mmol) was added gradually to pyridine (1 mL). The solution was mixed with egonol (40 mg, 0.12 mmol) dissolved in pyridine (1 mL). The reaction mixture was stirred at rt overnight. Subsequently, the reaction mixture was poured into water and extracted with ether, the organic phase was dried over anhydrous Na$_2$SO$_4$ and filtered, and the solvent was evaporated in vacuo. The residue was purified by CCC (petroleum ether−EtOAc; linear gradient from 1:0 to 2:3) to give **17** (35.0 mg, 84%).[27]

Preparation of 18 and 19. To a solution of **13** (20.0 mg, 0.061 mmol) in dry MeCN (2 mL) was added *tert*-butyl isocyanate (6.1 mg, 0.061 mmol) under argon. The reaction mixture was stirred and refluxed for 4 h. Subsequently, the solvent was evaporated in vacuo, the reaction residue was quenched with water (10 mL) and extracted with CH$_2$Cl$_2$ (15 mL × 3), the organic phase was dried over anhydrous

Na$_2$SO$_4$ and filtered, and the solvent was evaporated in vacuo. The residue was purified by CCC (heptane−EtOAc; linear gradient from 1:0 to 1:1) to give **18** (10.4 mg, 75%). Under similar conditions, **13** (20.0 mg, 0.061 mmol) was treated with phenyl isocyanate (7.4 mg, 0.06 mmol) in dry MeCN (1 mL) to yield **19** (27.3 mg, 98%).

Compound **18**: amorphous solid; UV (CH$_2$Cl$_2$) λ_{max} (log ε) 229 (4.24), 318 (4.34) nm; IR ν_{max} CH$_2$Cl$_2$ 2921, 2852, 1709, 1473, 363, 1222, 1033, 927 cm^{-1}; ^{1}H NMR (CDCl$_3$, 300 MHz) δ 7.37 (1H, dd, *J* = 8.2, 1.8 Hz, H-6′), 7.29 (1H, d, *J* = 1.7 Hz, H-2′), 6.93 (1H, d, *J* = 1.3 Hz, H-4), 6.84 (1H, d, *J* = 8.2 Hz, H-5′), 6.76 (1H, s, H-3), 6.58 (1H, d, *J* = 1.3 Hz, H-6), 5.97 (2H, s, OCH$_2$O), 4.62 (1H, brs, NH), 4.10 (2H, t, *J* = 6.5 Hz, H-3′′), 4.00 (3H, s, OCH$_3$), 2.72 (2H, t, *J* = 7.5 Hz, H-1′′), 1.94 (2H, dd, *J* = 7.5, 6.5 Hz, H-2′′), 1.30 (3H, s, H-4′′′), 1.30 (3H, s, H-6′′′), 1.29 (3H, s, H-5′′′); ^{13}C NMR data (CDCl$_3$, 75 MHz) δ 157.0 (C, C-1′′′), 156.3 (C, C-2), 148.2 (C, C-3′), 148.1 (C, C-4′), 144.9 (C, C-7), 142.7 (C, C-8), 137.4 (C, C-5), 131.2 (C, C-9), 124.9 (C, C-1′), 119.4 (CH, C-6′), 112.5 (CH, C-4), 108.8 (CH, C-5′), 107.6 (CH, C-6), 105.7 (CH, C-2′), 101.5 (CH$_2$, OCH$_2$O), 100.6 (CH, C-3), 63.8 (CH$_2$, C-3′′), 56.4 (CH$_3$, OCH$_3$), 50.4 (C, C-3′′′), 32.8 (CH$_2$, C-1′′), 31.4 (CH$_2$, C-2′′), 29.67 (CH$_3$, C-5′′′), 29.2 (CH$_3$, C-4′′′), 29.2 (CH$_3$, C-6′′′); MALDI-TOF-HRESIMS *m/z* 448.1733 [M + Na]$^+$ (calcd for C$_{24}$H$_{27}$NO$_6$Na, 448.1736).

Compound **19**: amorphous solid; UV (CH$_2$Cl$_2$) λ_{max} (log ε) 219 (4.30), 233 (4.20), 318 (3.04) nm; IR ν_{max} CH$_2$Cl$_2$ 3320, 2938, 1726, 1597, 1537, 1501, 1475, 1444, 1364, 1313, 929 cm^{-1}; ^{1}H NMR (CDCl$_3$, 300 MHz) of the major rotamer δ 10.81 (1H, brs, NH), 7.53 (2H, ddd, *J* = 8.2, 2.5, 1.5 Hz, H-4′′′ and H-8′′′), 7.37 (1H, dd, *J* = 8.2, 1.7 Hz, H-6′), 7.29 (1H, d, *J* = 1.7 Hz, H-2′), 7.26 (2H, ddd, *J* = 8.2, 7.4, 1.5 Hz, H-5′′′ and H-7′′′), 7.04 (1H, tdd, *J* = 7.4, 1.8, 1.5 Hz, H-6′′′), 6.94 (1H, d, *J* = 1.3 Hz, H-4), 6.84 (1H, d, *J* = 8.2 Hz, H-5′), 6.76 (1H, s, H-3), 6.59 (1H, d, *J* = 1.3 Hz, H-6), 5.98 (2H, s, OCH$_2$O), 4.20 (2H, t, *J* = 6.5 Hz, H-3′′), 4.00 (3H, s, OCH$_3$), 2.76 (2H, dd, *J* = 9.3, 6.5 Hz, H-1′′), 2.03 (2H, ddd, *J* = 12.7, 9.3, 6.5 Hz, H-2′′); ^{13}C NMR data (CDCl$_3$, 125 MHz) of the major rotamer δ 156.4 (C, C-2), 153.8 (C, C-1′′′), 148.3 (C, C-3′), 148.2 (C, C-4′), 145.0 (C, C-7), 142.7 (C, C-8), 138.1 (C, C-3′′′) 137.4 (C, C-5), 131.3 (C, C-9), 129.3 (CH, C-5′′′), 129.3 (CH, C-7′′′), 124.9 (C, C-1′), 123.6 (CH, C-6′′′) 120.2 (CH, C-8′′′), 120.2 (CH, C-4′′′) 119.4 (CH, C-6′), 112.6 (CH, C-4), 108.8 (CH, C-5′), 107.6 (CH, C-6), 105.8 (CH, C-2′), 101.5 (CH$_2$, OCH$_2$O), 100.6 (CH, C-3), 64.9 (CH$_2$, C-3′′), 56.4 (CH$_3$, OCH$_3$), 32.8 (CH$_2$, C-1′′), 31.2 (CH$_2$, C-2′′); MALDI-TOF-HRESIMS *m/z* 468.1419 [M + Na]$^+$ (calcd for C$_{26}$H$_{23}$NO$_6$Na, 468.1423).

In Vitro AChE and BChE Inhibition. Enzymes *Ee*AChE from *Electrophorus electricus* (ref C2888), recombinant *h*AChE from human (reference C1682), and *h*BChE from human serum (reference B4186) were purchased from Sigma. Inhibition of AChE activity was determined by the spectroscopic method of Ellman et al.,[28] using acetylthiocholine iodide as substrate, in 96-well microtiter plates. All solutions were brought to room temperature prior to use. Aliquots of 200 μL of a solution containing 640 μL of 10 mM 5,5′-dithiobis-2-nitrobenzoic acid (DTNB) in 0.1 M sodium phosphate, pH 8.0, 19.2 mL of the same buffer, and 13 μL of a solution of AChE (100 U/mL) in water were added to each well, followed by 2 μL of a DMSO solution of the inhibitor (0.9% final volume). The reaction was initiated by adding 20 μL of acetylthiocholine iodide (7.5 mM) to each well and was followed by monitoring the appearance of the thiolate dianion produced by reduction of DTNB at 412 nm every 13 s for 120 s at 25 °C in a Molecular Devices Max 384 Plus plate reader. Each inhibitor was evaluated at 10 concentrations (from 1 mg to 0.05 mg/mL by diluting by a factor 3). Percentage inhibition was calculated relative to a control sample of DMSO (% inhibition = [1 − (slope cpd/slope DMSO)] × 100) with SoftMax Pro software. IC$_{50}$ values displayed represent the means ± SD of three individual determinations each performed in triplicate assays. Tacrine hydrochloride (Sigma) was used as the reference compound.

Inhibition of BChE was measured as described above, substituting 100 U/mL of *h*BChE and 75 mM butyrylthiocholine iodide for enzyme and substrate, respectively.

Inhibition of AChE-Induced Aβ-Aggregation. To quantify amyloid fibril formation, the thioflavin T fluorescence method was applied.[29] Aliquots of 2 μL of β-amyloid$_{1-40}$ (Aβ1−40) peptide (Butendorf, Switzland), lyophilized from 2 mg/mL HFIP solution and dissolved in DMSO at a final concentration of 230 μM, were incubated for 24 h at rt (25 °C) in 0.215 M sodium phosphate buffer (pH 8.0). For co-incubation experiments, aliquots (16 μL) of *Ee*AChE from *Electrophorus electricus* (Sigma-Aldrich) (final concentration of 2.3 μM, Aβ/AChE molar ratio of 100:1) and *Ee*AChE in the presence of 2 μL of the tested inhibitors (final inhibitor concentration 100 μM) were added. Blanks containing Aβ, *Ee*AChE, Aβ plus inhibitors in 0.215 M sodium phosphate buffer (pH 8.0), and *Ee*AChE plus inhibitors in 0.215 M sodium phosphate buffer (pH 8.0) were prepared. The final volume of each vial was 20 μL. Each assay was run in duplicate. After incubation, the samples containing Aβ, Aβ plus AChE, or Aβ plus AChE in the presence of inhibitors were diluted with 50 mM glycine−NaOH buffer (pH 8.5) containing 1.5 μM thioflavin T (Sigma-Aldrich) to a final volume of 2.0 mL. For the thioflavin T-based fluorometric assay, analyses were performed with a Jasco spectrofluorimeter FP-750 using a 2 mL quartz cell. Fluorescence was monitored with excitation at 446 nm (λ_{exc}) and emission at 490 nm (λ_{em}). A time scan of fluorescence was performed, and the intensity values reached at the plateau (around 300 s) were averaged after subtracting the background fluorescence from 1.5 μM thioflavin T and AChE. The fluorescence intensities were compared, and the percent inhibition due to the presence of the test compounds was calculated. The percent inhibition of the AChE-induced aggregation due to the presence of the tested compound was calculated by the following expression: 100 − [IFi − IFc)/IFo × 100], where IFi, IFo, and IFc are the fluorescence intensities obtained for Aβ plus AChE in the presence and in the absence of inhibitor and the tested compound, respectively, after subtracting the fluorescence of respective blanks. In our testing procedure of thioflavin T, tested benzofuran analogues were found to be strong innately fluorescent compounds with two excitation wavelengths, at 336 and 470 nm (λ_{exc}), and two emission wavelengths, at 370 and 490 nm (λ_{em}). So the percent inhibition was calculated by subtracting their own fluorescence intensity of tested compounds.

Molecular Modeling. Molecular docking was carried out using GOLD 4.0[34] with standard parameters. The published crystal structure of *Ee*AChE (pdb code 1EEA) was used, with a binding site defined as a 20 Å radius sphere around the OH group of Ser200. The 3D structures of ligands were constructed with CORINA 3.44.[35] Molecular dynamics simulations were carried out with GROMACS version 4.0.2[36] using the OPLS-AA[37] force field. Each system was energy-minimized until convergence using a steepest descents algorithm. Molecular dynamics with position restraints for 200 ps was performed followed by the production run of 10 ns. During the position restraints and production runs, the Parinello−Rahman method[38] was used for pressure coupling, and the temperature was coupled using the Nosé−Hoover method[39] at 300 K. Electrostatics were calculated with the particle mesh Ewald method.[40] The P-LINCS algorithm[41] was used to constrain bond lengths, and a time step of 2 fs was used throughout. Ligand topologies for the OPLS-AA force field were obtained in a semiautomated manner using an in-house developed script. All calculations were performed using the high-performance computing (HPC) facilities at the ICSN. Images were generated with Chimera[42] and raytraced with the POV-ray module.

ASSOCIATED CONTENT

Ⓢ **Supporting Information.** NMR spectra of compounds **1**, **2**, **4**, **14**, **15**, **18**, and **19** and molecular dynamics simulations of compounds **1**−**6**. This material is available free of charge via the Internet at http://pubs.acs.org.

AUTHOR INFORMATION

Corresponding Author
*Tel: +33 1 69 82 30 38. Fax: +33 1 69 07 72 47. E-mail: vincent.dumontet@icsn.cnrs-gif.fr.

ACKNOWLEDGMENT

REFERENCES

(1) Walsh, D. M.; Selkoe, D. J. *Neuron* **2004**, *44*, 181–193.
(2) Ferri, C. P.; Prince, M.; Brayne, C.; Brodaty, H.; Fratiglioni, L.; Ganguli, M.; Hall, K.; Hasegawa, K.; Hendrie, H.; Huang, Y.; Jorm, A.; Mathers, C.; Menezes, P. R.; Rimmer, E.; Scazufca, M. *Lancet* **2005**, *336*, 2112–2117.
(3) DeKosky, S. T. *J. Am. Geriatr. Soc.* **2003**, *51*, 314–320.
(4) Parihar, M. S.; Hemnani, T. *J. Clin. Neurosci.* **2004**, *11*, 456–467.
(5) Bartus, R. T.; Dean, R. L.; Beer, B.; Lippa, A. S. *Science* **1982**, *217*, 408–414.
(6) Alvarez, A.; Bronfman, F.; Perez, C. A.; Vicente, M.; Garrido, J.; Inestrosa, N. C. *Neurosci. Lett.* **1995**, 49–52.
(7) Alvarez, A.; Opazo, C.; Alarcon, R.; Garrido, J.; Inestrosa, N. C. *J. Mol. Biol.* **1997**, *272*, 348–361.
(8) Inestrosa, N. C.; Alvarez, A.; Perez, C. A.; Moreno, R. D.; Vicente, M.; Linker, C.; Casanueva, O. I.; Soto, C.; Garrido, J. *Neuron* **1996**, *16*, 881–891.
(9) Jacobsen, J. S. *Curr. Top. Med. Chem.* **2002**, *2*, 343–352.
(10) Maia, A.; Schmitz-Alfonso, I.; Martin, M.-T.; Awang, K.; Laprévote, O.; Guéritte, F.; Litaudon, M. *Planta Med.* **2008**, *74*, 1–6.
(11) Beniddir, M. A.; Simonin, A.-L.; Martin, M.-T.; Dumontet, V.; Poullain, C.; Guéritte, F.; Litaudon, M. *Phytochem. Lett.* **2010**, *3*, 75–78.
(12) Fritsch, P. W. *Mol. Phylogenet. Evol.* **2001**, *19*, 387–408.
(13) Pauletti, P. M.; Teles, H. L.; Silva, D. H. S.; Araújo, Â. R.; Bolzani, V. S. *Braz. J. Pharmacogn.* **2006**, *16*, 576–590.
(14) Min, B. S.; Oh, S. R.; Ahn, K. S.; Kim, J. H.; Lee, J.; Kim, D. Y.; Kim, E. H.; Lee, H. K. *Planta Med.* **2004**, *70*, 1210–1215.
(15) Pauletti, P. M.; Araujo, A. R.; Young, M. C.; Giesbrecht, A. M.; Bolzani, V. D. *Phytochemistry* **2000**, *55*, 597–601.
(16) Bousserouel, H.; Litaudon, M.; Morleo, B.; Martin, M. T.; Thoison, O.; Nosjean, O.; Boutin, J. A.; Renard, P.; Sevenet, T. *Tetrahedron* **2005**, *61*, 845–851.
(17) Ozturk, S. E.; Akgul, Y.; Anil, H. *Bioorg. Med. Chem.* **2008**, *16*, 4431–4437.
(18) Takanashi, M.; Takisawa, Y. *Phytochemistry* **1988**, *27*, 1224–1226.
(19) Li, Q. L.; Li, B. G.; Qi, H. Y.; Gao, X. P.; Zhang, G. L. *Planta Med.* **2005**, *71*, 847–851.
(20) Park, S. Y.; Lee, H.-J.; Lee, O.-K.; Kang, H.-Y.; Choi, D.-H.; Paik, K.-H.; Khan, M. *Bull. Korean Chem. Soc.* **2007**, *28*, 1874–1876.
(21) Takanashi, M.; Takizawa, Y. *J. Oleo Sci.* **2002**, *51*, 151–155.
(22) Akgul, Y. Y.; Anil, H. *Phytochemistry* **2003**, *63*, 939–943.

(23) Takanashi, M.; Takizawa., Y.; Mitsuhashi, T. *Chem. Lett.* **1974**, *8*, 869–871.

(24) Aursand, M.; Grasdalen, H. *Chem. Phys. Lipids* **1992**, *62*, 239–251.

(25) Gunstone, F. D.; Jacobsberg, F. R. *Chem. Phys. Lipids* **1972**, *9*, 112–122.

(26) Gunstone, F. D. In *Advances in Lipid Methodology—Two*; Christie, W. W., Ed.; Oily Press: Dundee, 1993; Chapter 1, pp 1—68.

(27) Puentes de Diaz, A. *Phytochemistry* **1997**, *44*, 345–346.

(28) Ellman, G. L.; Courtney, K. D.; Andres, V., Jr.; Feather-Stone, R. M. *Biochem. Pharmacol.* **1961**, *7*, 88–95.

(29) Bartolini, M.; Bertucci, C.; Cavrini, V.; Andrisano, V. *Biochem. Pharmacol.* **2003**, *65*, 407–416.

(30) Howlett, D. R.; Perry, A. E.; Godfrey, F.; Swatton, J. E.; Jennings, K. H.; Spitzfaden, C.; Wadsworth, H.; Wood, S. J.; Markwell, R. E. *Biochem. J.* **1999**, *340*, 283–289.

(31) Rizzo, S.; Riviere, C.; Piazzi, L.; Bisi, A.; Gobbi, S.; Bartolini, M.; Andrisano, V.; Morroni, F.; Tarozzi, A.; Monti, J. P.; Rampa, A. *J. Med. Chem.* **2008**, *51*, 2883–2886.

(32) William, P.; Sorribas, A.; Howes, M.-J. *Nat. Prod. Rep.* **2011**, *28*, 48–77.

(33) Ackman, R. G.; Reston, M. E.; Gallay, L. R.; Vandenheuvel, F. A. *Can. J. Chem.* **1961**, *39*, 1956–1963.

(34) Verdonk, M. L.; Cole, J. C.; Hartshorn, M. J.; Murray, C. W.; Taylor, R. D. *Proteins* **2003**, *52*, 609–623.

(35) http://www.molecular-networks.com/products/corina (accessed on Sept 6, 2011).

(36) Hess, B.; Kutzner, C.; van der Spoel, D.; Lindahl, E. *J. Chem. Theory Comput.* **2008**, *4*, 435–447.

(37) Jorgensen, W. L.; Maxwell, D. S.; Tirado-Rives, J. *J. Am. Chem. Soc.* **1996**, *118*, 11225–11236.

(38) Parinello, M.; Rahman, A. *J. Appl. Phys.* **1981**, *52*, 7182–7190.

(39) Nosé, S. *Mol. Phys.* **1984**, *52*, 255–268.

(40) Essman, U.; Perela, L.; Berkowitz, M. L.; Darden, T.; Lee, H.; Pedersen, L. G. *J. Chem. Phys.* **1995**, *103*, 8577–8592.

(41) Hess, B. *J. Chem. Theory Comput.* **2007**, *4*, 116–122.

(42) Pettersen, E. F.; Goddard, T. D.; Huang, C. C.; Couch, G. S.; Greenblatt, D. M.; Meng, E. C.; Ferrin, T. E. *J. Comput. Chem.* **2004**, *25*, 1605–1612.